Short communication

The rate characteristics of lithium iron sulfide

E. Kendrick*, J. Barker, J. Bao, A. Świątek

Surion Energy Ltd., E1 Culham Science Centre, Abingdon, Oxfordshire, GU12 5EG, UK

ABSTRACT

The electrochemical rate properties of Li_2FeS_2 synthesized *via* a low cost solid state method have been investigated. Apparent diffusion coefficients calculated from EVS and GITT measurements show rate limitations upon charge with distinct differences between the iron redox and sulfur redox regions. These differences between the iron and sulfur redox reactions are not mimicked upon discharge. The apparent diffusion coefficients are greater upon discharge than charge and this is reflected in the rate capabilities as measured by galvanostatic discharge and charge measurements.

© 2010 Elsevier B.V. All rights reserved.

1. Introduction

With the ever increasing demand for high energy density, safe and low cost energy storage devices for the electric vehicle market, there is a drive towards new and alternative chemistries. Current technologies are based around the layered oxide cathode systems $LiMO_2$ (where M = Co, Ni, Mn) vs. graphite. These systems have been well documented and have limitations in terms of the safety and hence the ability to process these into large format cells [1,2]. Lithium iron phosphate cathode, $LiFePO_4$ (LFP) exhibits much better safety characteristics [3], however the energy density of the system is much reduced due to the requirement for carbon coating and small particles sizes. We have studied an alternative cathode system $Li_{2-x}FeS_2$. This low cost lithium ion cathode material lithium iron disulfide (Li_2FeS_2) offers distinct advantages over the other cathode materials especially in terms of specific capacity, energy density and safety.

Li_2FeS_2 possesses a layered structure as shown in Fig. 1, with the ideal structure having layers of octahedrally coordinated lithium between layers of edge sharing lithium and iron tetrahedral. There has been a several comprehensive studies of the material Li_2FeS_2 and its change in oxidation state upon charge and discharge, the conclusion is that there are two redox centers in this compound $Fe^{2+} \rightarrow Fe^{3+}$ and $S^{2-} \rightarrow 1/2(S_2)^{2-}$ [5,6,8,9]. The initial voltage plateau observed upon charge, at lower voltages is due to the iron

redox and the higher voltage plateau is attributed to the sulfur redox. Therefore due to this two electron transfer the cathode material has a theoretical capacity of $400\,mAh\,g^{-1}$, with average discharge voltage vs. Li of around 2.2 V. The specific energy density of this material is therefore $880\,mWh\,g^{-1}$ which far surpasses the energy density of any commercial lithium-ion cathode. The material has been studied previously in terms of an intermediate product formed in $Li//FeS_2$ rechargeable cells [4] such as the polymer high temperature cells [5,6] and in high temperature cells using a lithium halide eutectic electrolyte which operates at approximately $450\,°C$ [7]. The work described here investigates $Li_{2-x}FeS_2$ synthesized *via* a low cost solid state method which can be used as cathode in a rechargeable lithium ion system. This work details the rate limitations in the material using a variety of electrochemical test methods.

2. Experimental

Lithium iron sulfide has been made by a low cost solid state route using the low cost precursors FeS_2 and Li_2CO_3. The precursors are ball milled initially using a roller mill, pelletised and then fired at temperatures between 750 and $800\,°C$ for 9–12 h [10]. The pellets are removed from the furnace and then ball milled at 150 rpm for 2 h under argon to reduce the particle size. The resulting powder is sieved and classified. The phase purity of the material is analyzed using X-ray diffraction, the X-ray diffraction is obtained using a Siemans D5000 diffractometer, copper X-ray sources and Kα1 and Kα2 wavelengths, the pattern is obtained over a range 10–80° 2θ, with a step size of 0.05° 2θ over a period of 4 h. Ex situ X-ray diffraction was performed on Li_2FeS_2 at different states of charge by charging a $14.7\,cm^{-2}$ composite coating of Li_2FeS_2 to a specified voltage

* Corresponding author. Current address: Sharp Laboratories Europe, Edmund Halley Road, Oxford Science Park, Oxford, OX4 4GB, UK.
Tel.: +44 (0)1865 747711; fax: +44 (0)1865 747717.
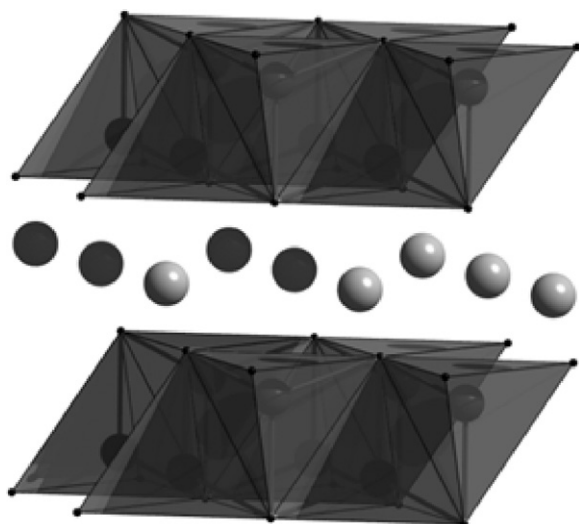*E-mail address:* emma8kendrick@gmail.com (E. Kendrick).

Fig. 1. The ideal structure of the Li_2FeS_2 phase, where the tetrahedral layers are occupied by Li and Fe ions in a ratio of 1:1, and the light grey spheres indicate octahedral lithium ions.

Fig. 2. X-ray diffraction pattern for Li_2FeS_2 synthesized *via* the proprietary solid state method, observed and calculated pattern from Batchelor et al. [8].

and then removing the charged cathode from the current collector in the glove box. A powder X-ray diffraction was performed on the resulting powder. The X-ray diffraction on the partially charged samples was performed on a Stoe STADI/P powder diffractometer with an Iron source in 0.7 mm glass capillary, 0.2 step, over 14 h.

Raman spectroscopy tests were performed on samples of charged active material, several powder samples were charged in a Swagelok® type cell with a lithium counter electrode. These cells did not contain any carbon black, and therefore an extremely low current rate of 10 mA g^{-1} was used to charge the cells to the specified voltage. The Raman spectroscopy was performed on a LEICA DMI 500 M in a 2 mm quartz capillary. Titration methods were used to calculate the Fe in the samples. A sample of Li_2FeS_2 was dissolved in sulfuric acid and this was titrated against potassium permanganate to calculate the levels of Fe^{2+} in the sample.

Electrochemical testing of the synthesized material was performed in a lithium metal test cells. Composite electrodes of active material, carbon black and a binder of polyethylene oxide (5 M) in DCM, were slurry coated onto aluminum current collector using the doctor blade technique. A ratio of 90/6/4 of active material/Carbon Black/PEO was used. The coatings were dried over night at 40 °C in a vacuum oven, and then calendared. Test cells of the Li_2FeS_2 were made using disks of these coatings and various electrochemical tests were performed.

Constant current cycling tests were performed using a commercial battery cycler (Maccor Inc., Tulsa, OK, USA). High-resolution electrochemical measurements were performed using the Electrochemical Voltage Spectroscopy (EVS) technique [11]. EVS is a voltage step method, which provides a high-resolution approximation to the open circuit voltage curve for the electrochemical system under investigation. The EVS step size was 10 mV and the critical current density <100 μA cm^{-2}. Rate tests were performed using a variety of discharge currents and a constant current charge to 2.65 V vs. lithium, and a subsequent constant voltage step limited by current to 5 mA g^{-1}. Galvanostatic intermittent titration technique (GITT) was performed using the Maccor battery tester and the apparent diffusion coefficient calculated and compared with those from the EVS technique.

3. Results

Li_2FeS_2 has been synthesized *via* a solid state method as detailed previously [10]. A good purity product was obtained with low lev-
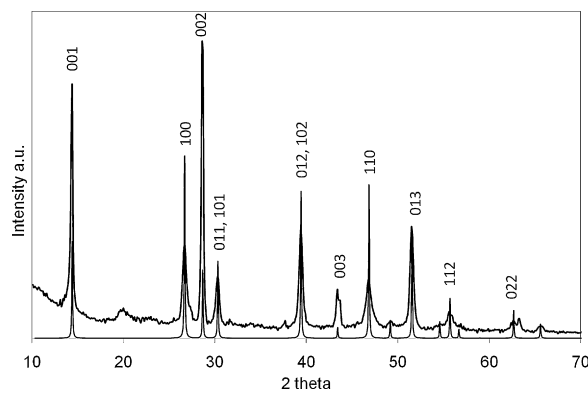
els of impurities as can be observed in Fig. 2. It can be observed that there is significant preferred orientation in the c axis as shown by the d_{hkl} 0 0 1 and 0 0 2 peaks at 14 and 29° 2θ respectively. Using the hexagonal space group *P-3m*1 as determined previously reported by Dahn et al., the cell parameters are found to be very similar to the fully lithiated material Li_2FeS_2 a = 3.9034(2) Å c = 6.3081(4) Å. Extremely low levels of impurities, which are likely to be sulfur, lithium sulfate and lithium sulfide are observed, these are incomplete reaction of the intermediate compounds formed during the reaction. These compounds were observed in larger quantities in less well reacted materials [10].

Fig. 3 shows the Raman spectroscopy of Li_2FeS_2 charged to several different voltages, it can be observed that there is no change in the oxidation state in the sulfur until the material is charged to above 2.45 V. This indicates no sulfur redox change in the lower voltage region and sulfur redox only on the higher plateau at 2.4 V vs. Li. This also indicates that the iron redox occurs at the lower voltage ranges and this has been previously confirmed by Mossbauer and IR experiments by Brec et al. [11,12].

The electrochemical voltage spectroscopy (EVS) voltage profile for Li_2FeS_2 vs. Lithium is shown in Fig. 4a. A reversible specific capacity of 320 mAh g^{-1} is observed. The initial charge voltage profile and the differential capacity plot (Fig. 4b) shows several defined features. Several small features occur at voltages less than 2.5 V vs. Li, these small peaks in the differential capacity plot are indicative of cation ordering due to the change in the iron oxidation state and
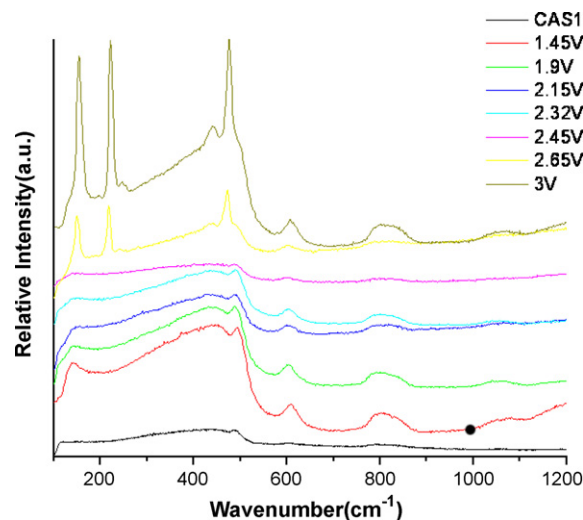

Fig. 3. Raman spectroscopy data for Li_2FeS_2 at increasing states of charge and decreasing degrees of lithiation.
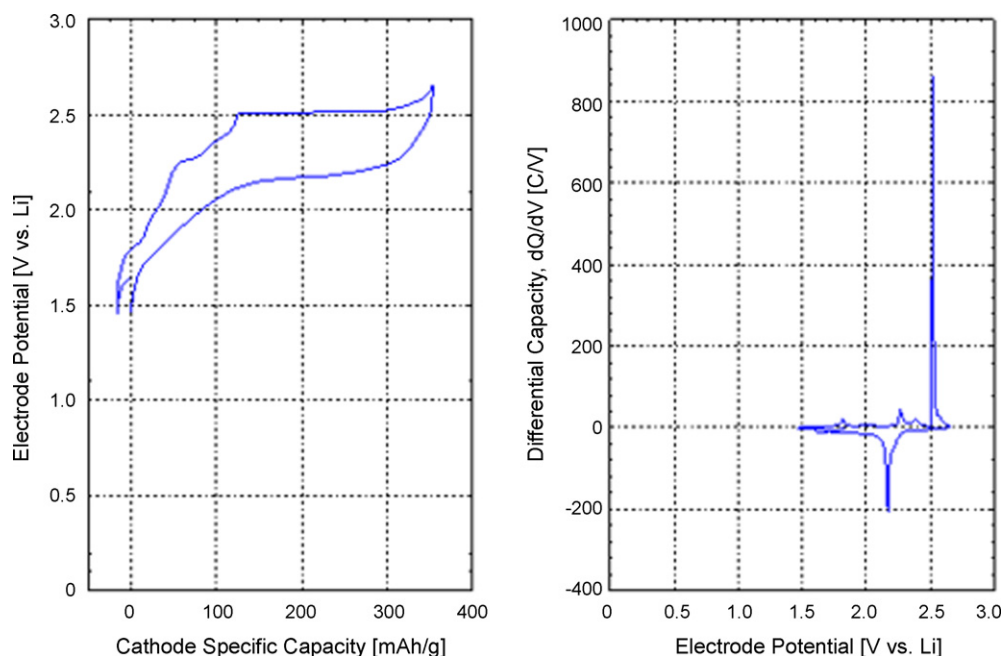
Fig. 4. First cycle EVS data for a representative Li//Li$_2$FeS$_2$ test cell. The cell was tested between voltage limits of 1.0 and 2.7V vs. Li using voltage steps of 10 mV and a limiting current density of 10 m Ag^{-1}. LHS: EVS voltage profile. RHS: EVS differential capacity profile.

environment as one lithium is extracted.

$$Li_2Fe^{2+}S_2 \rightarrow LiFe^{3+}S_2 + Li^+ + e^- \tag{1}$$

The larger flat plateau observed at 2.5 V is indicative of a 2 phase reaction region; this plateau is entirely due to the sulfur redox reaction $S^{2-} \rightarrow 1/2(S_2)^{2-}$.

$$LiFe^{3+}S_2 \rightarrow Fe^{3+}S^{2-}(S_2)_{1/2}{}^{2-} + Li^+ + e^- \tag{2}$$
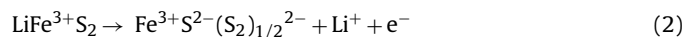
The X-ray diffraction pattern (shown in supplementary data) of Li$_2$FeS$_2$ at different states of charge, shows the peak at 34° 2θ disappears upon charge, and the peak at 76 increases. The sample was discharged to 1.45 V vs. Li, as can be observed the X-ray diffraction pattern is much less noisy, the peaks are much sharper. This indicates that there is probable cation disorder in the Li$_2$FeS$_2$ sample and upon initial lithium insertion a greater degree of order is achieved. Further work using neutron diffraction studies is required to study the lithium and iron ordering in more detail. As the material is charged most peaks shifted to larger angles and become broader; the peaks at ∼51° and ∼61° gradually disappear. There is a small peak observed at 76° 2θ after charging to 2.45 V, this is an indication that there may be the start of a two phase region, higher resolution data is required to investigate this further.

It is interesting to note that the top plateau is half of the theoretical capacity (200 mAh g^{-1}) which corresponds to 1 electron transfer. Since the material is highly water sensitive and the iron region is the lowest voltage region, the iron redox occurs preferentially for any delithiation which occurs during the handling of the electrode materials. It also indicates that if the material is not fully lithiated during synthesis the charge balance is maintained by the iron redox. The indication from initial wet chemistry methods is that the level of Fe^{III} is negligible in the active material, in order to understand this in more detail iron Mossbauer is required.

The Galvanostatic intermittent titration technique was used to investigate the observed polarization in the Li$_{2-x}$FeS$_2$ cathode material upon lithium extraction and reinsertion. As is shown in Fig. 5, at low levels of lithium extraction where $x < 0.75$ the polarization is much reduced compared to that with high levels of lithium extraction ($x > 0.75$). This indicates that the sulfur redox reaction is limited compared to the iron redox, and this may hinder the

rate capability of Li$_2$FeS$_2$ upon charge. However upon discharge the polarization appears to be very similar for all levels of lithium content. The sloping voltage curve indicates a probable solid solution of lithium in Li$_{2-x}$FeS$_2$ rather than a 2 phase region which corresponds well to the similar polarization observed over the whole region.

The apparent diffusion coefficients have been calculated from EVS and GITT measurements, both methods give initial charge apparent diffusion coefficients with the same order of magnitude of diffusion (Figs. 6 and 7). It can be observed that upon charge there are 4 separate peaks in the apparent diffusion coefficient relating to lithium ion diffusion in the low voltage iron redox region. At higher levels of lithium extraction both the EVS and GITT techniques show very slow apparent diffusion coefficients. In the GITT measurements the open circuit voltage must be reached in order to calculate the apparent diffusion coefficient, however in the EVS techniques the current transient is fitted to a Cottrell curve, and therefore in slow reactions, as observed here, the EVS measurements give a
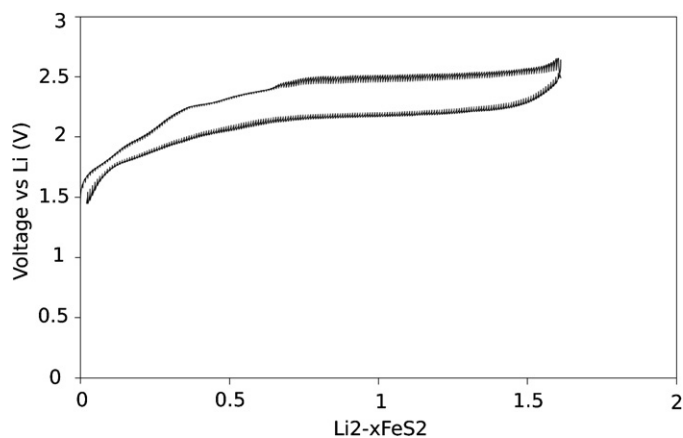

Fig. 5. GITT voltage profile with steps of 10 min charge or discharge and 1 h rest to open circuit voltage steps for charge and discharge. Low polarization regions are observed in the iron redox region upon charge and high in the sulfur redox regions, upon discharge a similar level of polarization is observed.
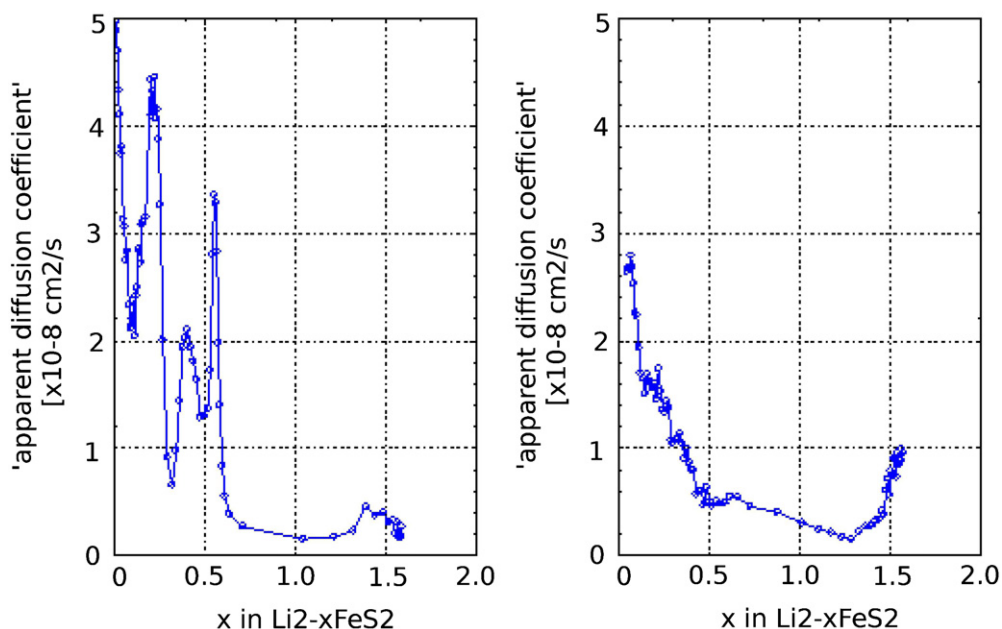
Fig. 6. Apparent diffusion coefficient data calculated from the EVS data: LHS = charge; RHS = discharge.

better approximation of the apparent diffusion coefficients. The slow apparent diffusion coefficient observed in the EVS data can be correlated to the sulfur redox reaction region, as discussed, this may limit the charge rate of this cathode material. Upon discharge and lithium insertion there are no observed fast apparent diffusion coefficient peaks, instead an overall similar diffusion coefficient for all levels of x which is greater than the charge at high levels of lithium extraction. The possible solid solution phase formed upon discharge as is indicated by the sloping voltage profile observed in the GITT and EVS graphs, (Figs. 4 and 5), require further examination by higher resolution techniques such as neutron diffraction.

The rate capabilities of the Li_2FeS_2 material was tested using a variety of charge and discharge rates ranging from 0.1 C (30 mAh g^{-1}) to 2 C (600 mAh g^{-1}) however the charge capability at 2 C was extremely poor and so the graph in Fig. 8 shows only rates

up to 300 mAh g^{-1} for comparison. It can be observed that upon discharge 85% of the initial capacity at 0.1 C is achieved whilst upon charge only 25% of the initial capacity is reached. This is likely due to the slow apparent diffusion coefficients observed on the upper plateau and the sulfur redox.

4. Discussion/conclusion

The electrochemical properties of Li_2FeS_2 synthesized *via* a solid state method have been investigated. The observed apparent diffusion coefficients calculated from EVS and GITT measurement indicate that the rate capabilities upon discharge are much greater than that upon charge and this is also observed in the signature curves for charge and discharge rates up to C rate (300 mAh g^{-1}).
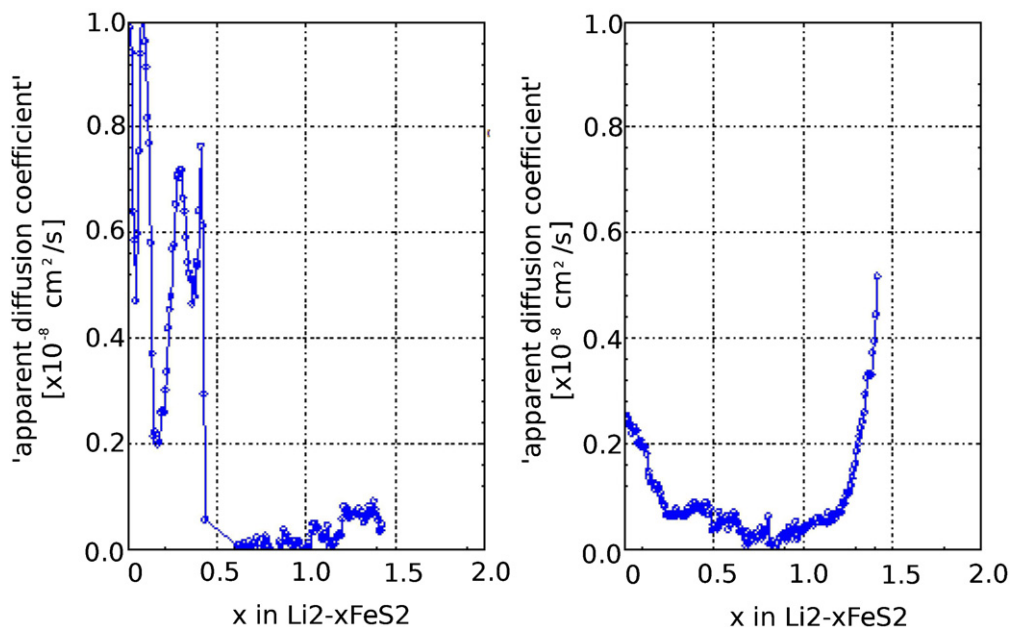

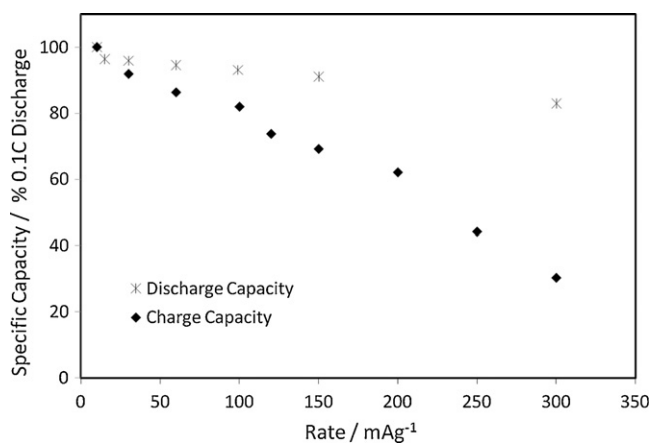**Fig. 7.** Apparent diffusion coefficient data calculated from the GITT data: LHS = charge; RHS = discharge.

Fig. 8. Charge and discharge signature curves for $Li_{2-x}FeS_2$, discharge rate capability is significantly greater than the charge rate capability.

The difference in the apparent diffusion coefficients are due to the difference in the cation positions and the probable formation of a solid solution of the lithium over the whole voltage range upon discharge compared to the distinct low voltage and high voltage regions upon charge. Upon charge the two regions relate to the low polarization of the iron redox reaction at low voltages and the high polarization at 2.5 V vs. Li from the sulfur redox reaction.

These results indicate that significant attention to the changes in crystal structure and lithium environment must be taken into consideration when optimizing this low cost cathode material for rate applications.

Appendix A. Supplementary data

Supplementary data associated with this article can be found, in the online version, at doi:10.1016/j.jpowsour.2010.11.158.

References

[1] J.R. Dahn, E.W. Fuller, M. Obrovac, U. Von Sacken, Solid State Ionics 69 (1994) 265–270.
[2] A. Arora, N.K. Medora, T. Livernois, J. Swart, Elect. Hybrid Vehicle (2010) 463–491.
[3] K. Zaghib, P. Charest, A. Guerfi, J. Shim, M. Perrier, K. Striebel, J. Power Sources 146 (2005) 380–385.
[4] A.N. Jansen, Encycl. Electrochem. Power Sources (2009) 145–150.
[5] E. Strauss, D. Golodnitsky, K. Freedman, A. Milner, E. Peled, J. Power Sources 115 (2003) 323–331.
[6] D. Golodnitsky, E. Peled, Electrochim. Acta 45 (1999) 335–350.
[7] P.J. Masset, R.A. Guidotti, J. Power Sources 177 (2009) 145–150.
[8] R.J. Batchelor, F.W.B. Einstein, C.H.W. Jones, R. Fong, J.R. Dahn, Phys. Rev., Ser.: B – Condens. Matter 37 (1988) 3699–3702.
[9] L. Blandeau, G. Ouvrard, Y. Calage, R. Brec, J. Rouxel, J. Phys. C 20 (1987) 4271–4281.
[10] 'Lithium containing metal sulphide compounds' UK Patent GB2464455B.
[11] R. Brec, E. Prouzet, G. Ouverard, J. Power Sources 26 (1989) 325–332.
[12] P. Gard, C. Sourisseau, G. Ouverard, Solid State Ionics 20 (1980) 231–238.